Geologie en Mijnbouw **73:** 235–240, 1994.

The seismic activity near Aachen following the 1992 Roermond earthquake, the Netherlands

D. Prinz, D. Hollnack & J. Wohlenberg
Lehr- und Forschungsgebiet für Angewandte Geophysik der Rheinisch-Westfälische Technische Hochschule Aachen, Lochnerstr. 4–20, 52064 Aachen, Germany

Received 6 June 1993; accepted in revised form 18 February 1994

Key words: aftershocks, fault-plane solutions, Lower Rhine Embayment, seismotectonic source parameters

Abstract

The seismic activity following the large Roermond earthquake of April 13, 1992, was concentrated in the area of the main shock and, surprisingly, a few kilometers northeast of Aachen. The locations and source parameters of 13 earthquakes, which occurred in the Aachen area, are presented. The evaluation is based mainly on seismograms from four mobile seismograph stations of the RWTH Aachen (Rheinisch-Westfälische Technische Hochschule) which were installed close to the epicenters. Fault-plane solutions were determined for two of these earthquakes.

Introduction

After the large Roermond earthquake of April 13, 1992, working groups from several European countries started to install a dense network of recording stations in order to monitor the aftershock activities (Camelbeeck et al. 1994). From the morning of April 13 until September 7, 1992, the Geophysics Department of the Rheinisch-Westfälische Technische Hochschule (RWTH) Aachen operated four mobile seismograph stations, covering the Aachen area in this network.

Though aftershock activity near Roermond is to be expected, it was surprising that the seismicity northeast of Aachen, more than 50 km away from the main shock, increased remarkably. The seismic recordings of the RWTH mobile stations offered almost ideal conditions to evaluate these events since they were positioned close to the epicenters.

Instrumentation and station distribution

The seismic units installed were of Lennartz PCM-5800 type, equipped with 1 Hz, three-component Mark L-4C 3D seismometers. Digital tape recording with a sampling-rate of 200 Hz was used to store the data. To avoid aliasing, low-pass filters with a limiting frequency of 43 Hz were applied. The time base was provided by DCF-receivers.

Between April 13 and September 7, 1992, the instruments recorded 25 events with local magnitudes, M_L, varying between 0.4 and 3.8 in the area around Aachen. In addition to the data from the RWTH stations, records from the station networks of the Geological Survey of Northrhine-Westphalia (GSH, OLF), the University of Cologne (DRE, SBR) and the Belgian network (EBN, MEM) were used to locate the events (Fig. 1).

Stations ACS1 and ACS2 were located on the Palaeozoic basement (Devonian), station ACS3 on the Cretaceous-Tertiary boundary, and stations ACS4 and ACS5 on Tertiary layers with different thicknesses.

Event location

Program HYPOCENT (Lienert et al. 1986) was used for locating the events. The assumed velocity-depth model as proposed by Ahorner (1983) and modified by Budny (1985) for the Rhine embayment and its foreland is shown in Fig. 2. Budny (1985), who used the research borehole Konzen (approximately 25 km S of Aachen) for a velocity study in the Palaeozoic basement, suggested only minor changes. The V_p/V_s-ratio

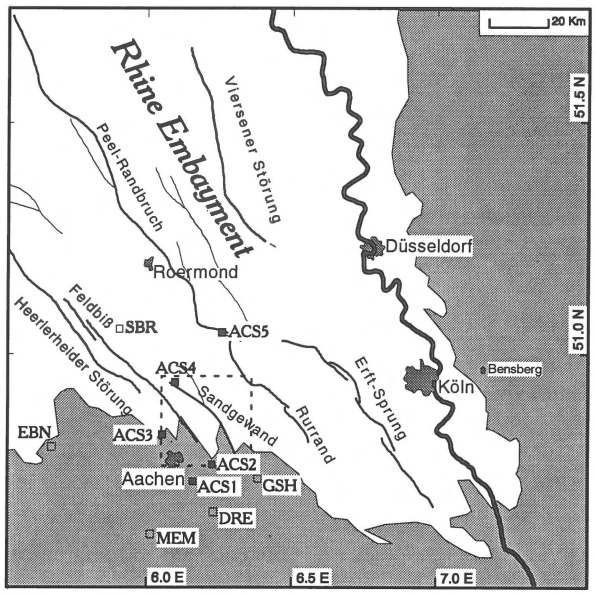

Fig. 1. Stations used for locating the 13 events (station OLF is situated outside this map, nearly 40 km SE of Aachen). ■ = RWTH stations, □ = other stations. The dashed lines depict the area in Fig. 4. Grey indicates the Rhenish Massif; major faults are named in German and indicated with solid lines.

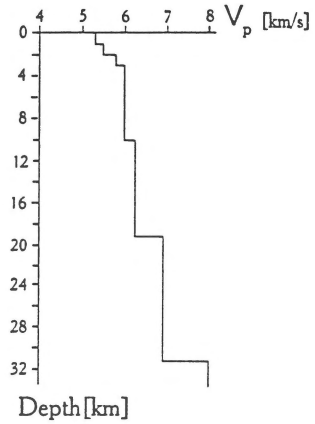

Fig. 2. Assumed velocity-depth model for the lower Rhine Embayment modified after Ahorner (1983) and Budny (1985).

had to be changed from 1.69 to 1.73 and the P-velocity increased from 5.0 to 5.3 km/s for the uppermost layer.

Additional modifications of the velocity model were necessary for the recording sites ACS4, ACS5 and SBR because of the thick Tertiary layers they were placed on. To correct for the time-delays of P- and S-arrivals, three-layer models were developed for each of the three sites considering a sedimentary cover of 450, 1450 and 1000 m for the stations ACS4, ACS5 and SBR respectively. The seismic velocities of the Tertiary cover were modelled following Budny (1984), who determined P- and S-wave velocities in the Tertiary layers of the Rhine embayment. In Fig. 3 the stratigraphic sequence of the Tertiary at station ACS5 and the corresponding velocity-depth model are given as an example.

The lengths of the ray paths within the sediments under each station were determined from the angle of incidence as found from the particle motion of the three-component seismograms. Using the velocity-depth models for the different stations we calculated the time delays with respect to the assumed regional velocity model. With these assumptions, 13 events of the recorded 25 around Aachen were located (Table 1). Obtained focal depths vary between 12 and 18 km. The concentration of events west of Eschweiler with focal depths of about 16 to 17 km is noteworthy.

Figure 4 depicts the obtained epicenters within the local tectonic setting. The strongest recorded event near Aachen, $M_L = 3.8$, was located 5 km southeast of Geilenkirchen.

Source parameters

For the located events dynamic source parameters, such as the seismic moments, M_o, fault radii, r, and the static stress drops, $\Delta\sigma$, were determined from the SH-displacement spectra using the Brune source model (Brune 1970). As an example, Fig. 5a shows the three-component seismograms of event 12 (Table 1) at station ACS1. The SH-displacement spectrum in Fig. 5b is determined from the E-W component of this recording.

The time series were first corrected for the instrument response and band-pass filtered between 1 and 80 Hz. The obtained displacement data were used to perform a Fast-Fourier Transform using 1 second windows with 10% cosine-bell shaped ends. The absorption factor Q = 500 was used for the stations on the Palaeozoic basement and Q = 200 for those on the Tertiary sediments. From the obtained ground displacement spectra, corner frequencies between 5 and 28 Hz were determined, resulting in estimates of r varying between 50 and 250 m. The estimated M_o varied between $3.7.10^{10}$ and $2.8.10^{14}$ Nm. Based on these results we obtained $\Delta\sigma$ between 0.08 and 7.9 MPa. Figure 6 summarizes the estimated source parameter

Depth[m]	Stratigraphical Unit	Stage, System	Velocity[km/s]
100 200	Reuverton, Rotton, Hauptkiesserie	Pliocene, Tertiary	v_p:1.95 v_s:0.81
300 400 500 600 700	Indener Schichten, Ville Schichten	Miocene, Tertiary	v_p:2.25 v_s:1.0
800 900 1000 1100 1200 1300	Grafenberger Schichten, Lintforter Schichten, Ratinger Schichten, Walsumer Schichten, Gereonsweiler Schichten, Ratheimer Schichten	Oligocene, Tertiary	v_p:2.35 v_s:1.16
1400	Merksteiner Schichten, Alsdorfer Schichten	Westfal B, Carboniferous	v_p:5.3 v_s:3.06

Fig. 3. Model of the velocity distribution in the Tertiary cover at station ACS5 based on Budny (1984).

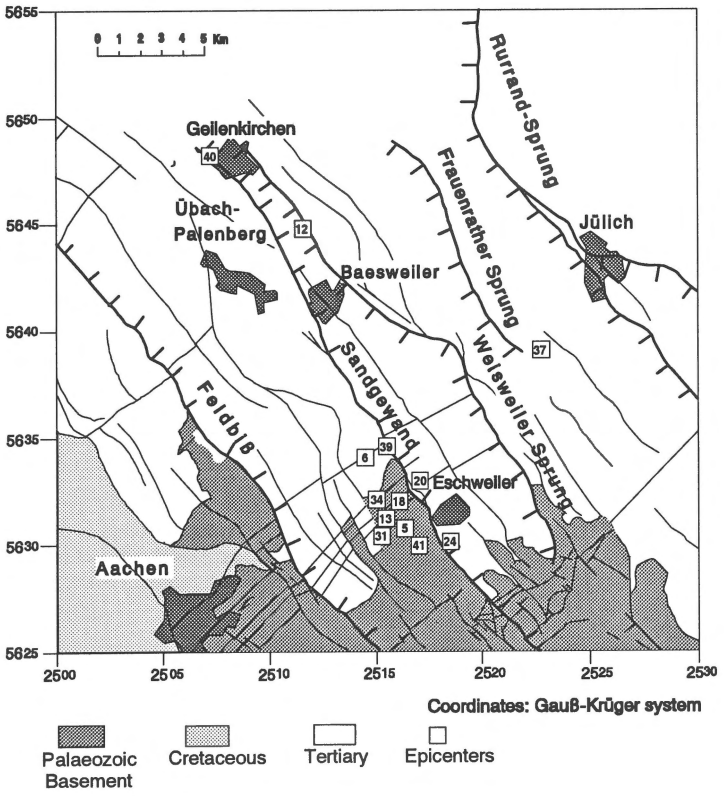

Fig. 4. Epicentral distribution of the earthquakes near Aachen, April–August 1992 (squares with numbers, which refer to the events listed in Table 1). Fault-plane solutions for events 12 and 13 are given in Fig. 7.

Table 1. Data and source parameters of 13 aftershocks located in the vicinity of Aachen, Germany

Ev.	Date	Time (GMT)	Lat. N (°)	Long. E (°)	Depth (km)	Mag	No	RMS (s)	f_c (Hz)	r (km)	Moment (Nm)	Stress drop (MPa)
5	13.04.	18:34	50.8128	6.2324	17.61	1.0	5	0.02	11.0	0.110	1.70E+12	0.56
6	13.04.	18:46	50.8442	6.2040	12.25	0.9	3	0.21	18.0	0.065	5.50E+10	0.09
12	14.04.	01:06	50.9405	6.1650	16.74	3.8	20	0.05	5.8	0.250	2.80E+14	7.90
13	14.04.	01:36	50.8158	6.2190	17.53	2.9	14	0.05	6.7	0.195	3.40E+13	2.02
18	15.04.	22:05	50.8240	6.2268	17.29	1.5	6	0.03	15.0	0.090	5.00E+11	1.26
20	16.04.	00:05	50.8318	6.2422	16.41	0.8	3	0.04	18.0	0.065	2.40E+11	0.39
24	17.04.	23:56	50.8070	6.2622	16.25	1.1	3	0.07	28.0	0.045	3.70E+10	0.18
31	20.04.	16:50	50.8108	6.2165	17.24	2.0	10	0.06	13.0	0.103	2.50E+12	1.06
34	26.04.	01:45	50.8245	6.2132	17.32	1.3	5	0.02	12.0	0.108	4.40E+12	1.52
37	17.05.	09:26	50.8890	6.3237	14.44	2.0	8	0.13	13.5	0.097	1.40E+12	0.68
39	08.06.	02:17	50.8478	6.2202	16.26	0.6	3	0.03	23.0	0.060	1.00E+11	0.20
40	25.06.	16:48	50.9715	6.1028	13.43	2.5	3	0.08	15.0	0.087	1.20E+11	0.08
41	22.08.	02:46	50.8057	6.2427	17.07	0.4	3	0.05	24.0	0.059	6.00E+10	0.13

Ev – Event; Mag – Local magnitude; No – Number of stations which have recorded the event; RMS – Root Mean Square error as obtained in the location procedure; f_c – corner frequency; r – source radius.

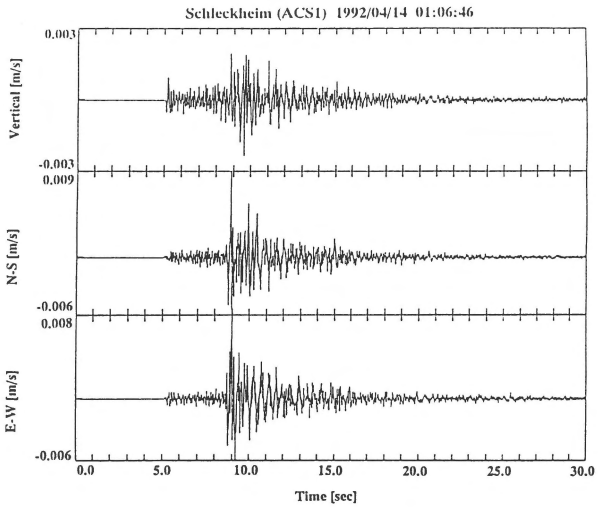

Fig. 5 a. Example of a seismogram: Event 12 (Table 1) recorded at station ACS1.

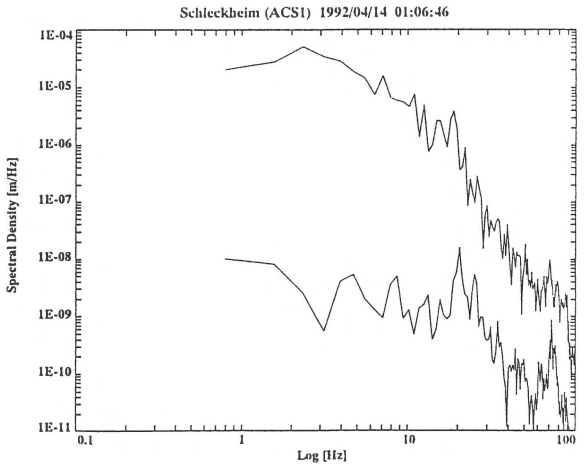

Fig. 5 b. SH-wave ground displacement spectrum of the E-W trace of the seismogram shown in Fig. 5a. The lower spectrum indicates the ground displacement noise.

in a log-log plot. The source radius, r, increases only slightly with increasing M_0 which is not surprising for the given moment range (11 of the 13 events have an $M_0 < 10^{13}$ Nm). This observation corresponds with several other investigations (Fletcher et al. 1986, Kim et al. 1989, Fletcher & Boatwright 1991) in which a nearly constant source radius over a large moment range has been ascertained for events with $M_0 < 10^{13}$ Nm.

Fault-plane solutions

Using all available first motion readings, including readings of stations operated by the Belgian and Dutch working groups, fault-plane solutions were determined for two events (Fig. 7). Both solutions show tensional dip-slip mechanisms with NW-SE striking fault-planes. These results are in good agreement with the

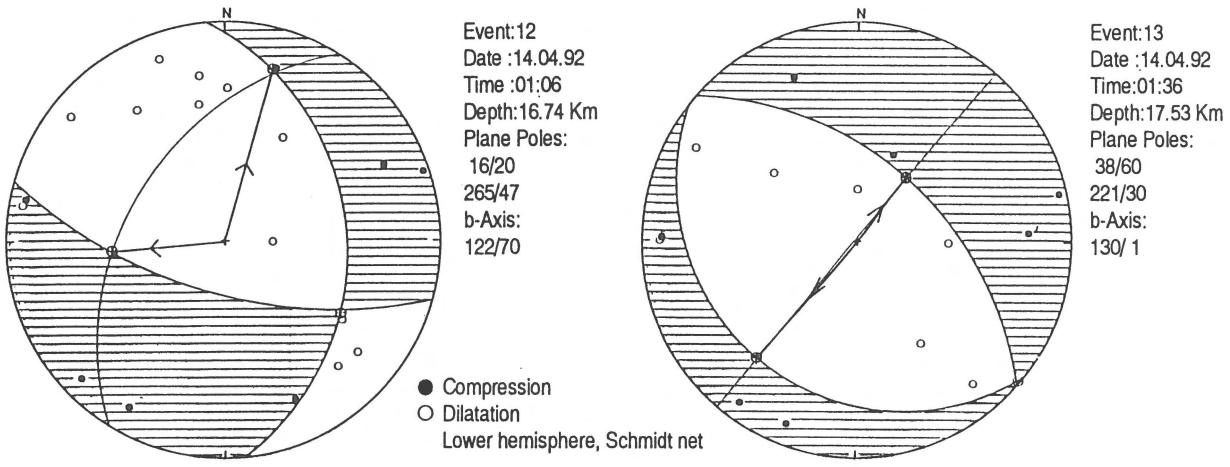

Fig. 7. Fault-plane solutions of two events located near to Aachen. The event numbers refer to Table 1. The hatched areas indicate P-wave first motion compression, the blank areas P-wave dilatation.

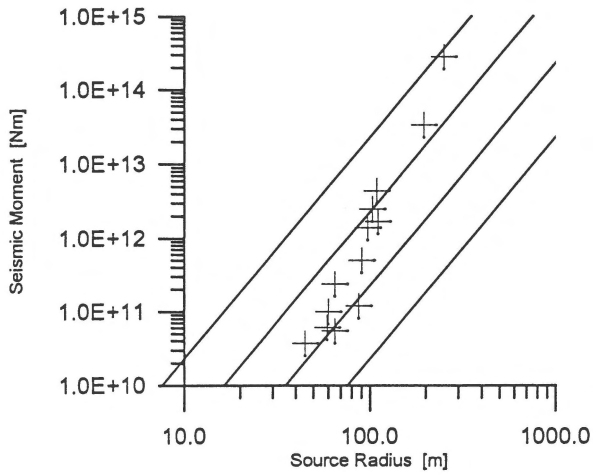

Fig. 6. Log-log plot of seismic moment M_o versus source radius for the 13 aftershocks listed in Table 1. Lines of constant stress drop $\Delta\sigma$ (0.01, 0.1, 1 and 10 MPa) are also drawn.

observed surface features and the seismotectonic investigations by Ahorner (1983) and Ahorner et al. (1983). The fault-plane solution of event 13 with a focal depth of more than 17 km suggests that it occurred on the Feldbiss Fault. Event 12 can be related to the Sandgewand Fault system, one of the major Quaternary faults in the active structural zone on the southwestern border of the Lower Rhine Graben.

Conclusions

The large energy release of the M_L=5.9 Roermond earthquake on April 13, 1992, triggered a remarkable increase of the seismic activity northeast of Aachen during the following weeks. Thirteen events with $0.4 \leq M_L \leq 3.8$ could be located with high accuracy. The strike directions of the fault planes as well as the focal mechanisms of the determined fault-plane solutions agree well with the results of other seismotectonic investigations in this area (Ahorner 1983, Ahorner et al. 1983). The estimated source parameters are showing well-known features as far as the relations between source radii, seismic moment and stress drop are concerned. The observed seismicity and the obtained source parameters reveal that the structural zone between the Eifel part of the Rhenish Massif and the Lower Rhine Embayment still carries a high seismic potential.

References

Ahorner, L. 1983 Historical Seismicity and Present-Day Microearthquake Activity of the Rhenish Massif, Central Europe. In: K. Fuchs et al. (ed.) Plateau Uplift. Springer-Verlag, Berlin: 198–221

Ahorner, L., B. Baier & K.-P. Bonjer 1983 General Pattern of Seismotectonic Dislocation and the Earthquake – Generating Stress Field in Central Europe between the Alps and the North Sea. In: K. Fuchs et al. (ed.) Plateau Uplift. Springer-Verlag, Berlin: 187–197

Brune, J. 1970 Tectonic stress and spectra of seismic shear waves from earthquakes – J. Geophys. Res. 75: 4997–5009

Budny, M. 1984 Seismische Bestimmung der bodendynamischen Kennwerte von oberflächennahen Schichten in Erdbebengebieten der Niederrheinischen Bucht und ihre ingenieurseismologische Anwendung – Ph.D. Thesis Universität Köln

Budny, M. 1985 P-Wave and SH-Wave Experiments in the Research Borehole Konzen, Hohes Venn (West Germany) – N. Jb. Geol. Paläont. Abh. 171: 105–115

Camelbeeck, T., T. van Eck, R. Pelzing, L. Ahorner, J. Loohuis, H.W. Haak, P. Hoang-Trong & D. Hollnack 1994 The 1992 Roermond earthquake, the Netherlands, and its aftershocks – Geol. Mijnbouw, this issue

Fletcher, J.B., L.C. Haar, F.L. Vernon, J.B. Brune, T.C. Hanks & J. Berger 1986 The effects of attenuation on the scaling of source parameters for earthquakes at Anza, California – In: Das, S., T. Boatwright & C. Scholz (eds) Earthquake Source Mechanics, American Geophysical Union, Geophys. Monogr. 37: 331–338

Fletcher, J.B. & J. Boatwright 1991 Source Parameters of Loma Prieta Aftershocks and Wave Propagation characteristics along the San Francisco Peninsula from a joint inversion of digital seismograms – Bull. Seism. Soc. Am. 81: 1783–1812

Kim, W.Y., R. Wahlström & M. Uski 1989 Regional spectral scaling relations of source parameters for earthquakes in the Baltic Shield. In: D. Denham (Ed.) Quantification of Earthquakes and the Determination of Source Parameters – Tectonophysics 166: 151–161

Lienert, R.B., E. Berg & L.N. Frazer 1986 HYPOCENTER: An earthquake location method using centered, scaled and adaptively damped least squares – Bull. Seism. Soc. Am. 76: 771–783